Ukrainian Journal of Physical Optics
ISSUE 1
2025

LOW-TEMPERATURE LUMINESCENCE OF LiB_3O_5 GLASS WITH A HUMAN BODY TISSUE-EQUIVALENT EFFECTIVE ATOMIC NUMBER

V. ADAMIV[1,*], YA. BURAK[1], I. MEDVID[2], I. KOFLYUK[2], U. DUTCHAK [3], I. TESLYUK[1], T. IZO[3], R. GAMERNYK [4]

[1] O.G.Vlokh Institute of Physical Optics of the Ivan Franko National University of Lviv, Dragomanov 23, 79005 Lviv, Ukraine.
[2] Ivan Franko National University of Lviv, Dragomanov 50, 79005, Lviv, Ukraine
[3] Lviv Oncology Regional Medical & Diagnostic Center, Ya. Hashek 2a, 79058 Lviv, Ukraine
[4] Ivan Franko National University of Lviv, Kyrylo & Mephodiy 8, 79005 Lviv, Ukraine.
*Corresponding author: vol.adamiv@gmail.com

Received: 22.10.2024

Abstract. A study of the low-temperature (8.6 K) luminescence of undoped LiB_3O_5 glass under excitation by synchrotron radiation (22.2 eV and 7.1 eV) was carried out. A comparative analysis of the obtained results was carried out with the results of studies of the low-temperature luminescence of undoped LiB_3O_5 single crystals published by other authors. As a result, a mechanism for the emission of undoped LiB_3O_5 glass at low temperatures was proposed, which is associated with the formation of unrelaxed molecular-type excitons, their migration, followed by the formation of autolocalized excitons near point defects, and with the corresponding their annihilation.

Keywords: lithium triborate glass, photoluminescence, synchrotron radiation, dosimetry
UDC: 535.37
DOI: 10.3116/16091833/Ukr.J.Phys.Opt.2025.01001

1. Introduction

Radiation therapy using gamma radiation has been used in medical practice for the treatment of cancer for a long time and has been quite successful. However, in radiation therapy for all types of radiation, the most important point is the accuracy of determining the doses received by of the patient's body. The accuracy of dose determination depends significantly on the material of the sensing element of the dosimeter. That is, it depends on how close the effective atomic number Z_{eff} of the dosimeter's sensing element is to the human body. As it turned out, for the borate compound LiB_3O_5, Z_{eff} = 7.39 [1,2], which is the closest to the value of human body tissue - Z_{eff} = 7.42.

The development of radiation therapy in modern medical practice requires visualizing the spatial distribution of radiation dose in the human body's tissues. This requires new special dosimeters to obtain information on the distribution of radiation dose both on the surface (2D) and in the volume (3D) of the body [3-5]. Such 2D and 3D dosimeters can be most successfully realized based on the phenomenon of optically stimulated luminescence (OSL) or radiophotoluminescence (RPL) [6-9].

Since the efficiency of dosimeters, including those based on OSL and RPL, is determined by the material of their working element, researchers are currently paying considerable attention to borates in the form of polycrystals [10], single crystals [11], glass [12], and glass ceramics [13]. The most promising borate for OSL and RPL dosimetry in medical practice may be lithium

triborate glass and glass ceramics LiB_3O_5 due to its tissue-equivalent Z_{eff} [2,12].

The advantage of LiB_3O_5 glass is the low cost of the starting reagents Li_2CO_3 and H_3BO_3 for synthesizing the compound and the increased tendency to form glass due to the high content of boron oxide B_2O_3. This ensures lower temperatures (in the range of 1200 – 1300 K) when producing LiB_3O_5 glass. It is also worth mentioning that in the manufacture of glass, there are practically no concentration limits for impurities and it becomes possible to more easily ensure their uniform distribution in the bubble volume. Our recent work [12] also showed that silver-doped lithium triborate glass LiB_3O_5:Ag can be very promising for γ-dosimetry in medical practice during radiation therapy of patients with cancer. Further research is necessary to optimize the conditions for glass obtaining, the activator's concentration, and the irradiation doses' value to obtain a glass dosimeter more sensitive to radiation. However, for a better understanding of the effect of the dopant on the luminescent parameters of doped LiB_3O_5 glass, it is worthwhile to study its luminescent properties in the undoped state in more detail. This is especially interesting because a series of articles have been published in the literature with the results of fundamental studies of the luminescent properties of undoped LiB_3O_5 single crystals in a very wide temperature range (7 – 500 K) [14-16]. In the following years, up to the present day, the authors have no information on the study of undoped polycrystals, single crystals, and LiB_3O_5 glass.

This paper presents the results of studies of the absorption, excitation spectra, and photoluminescence of undoped LiB_3O_5 glass at 8.6 K. It has also performed a comparative analysis with the results for single crystals of LiB_3O_5.

2. Materials and methods

High-purity lithium carbonate Li_2CO_3 and boric acid H_3BO_3 were the starting materials. The reagents were mixed in a certain proportion of LiB_3O_5 compound, and the solid-state reaction method was used to synthesize a ceramic crucible at 973 K. As a result of the chemical reaction:

$$Li_2CO_3 + 6H_3BO_3 \rightarrow 2LiB_3O_5 + CO_2 + 9H_2O,$$

LiB_3O_5 charge was obtained in the form of a powder with T_{melt} = 1107 K. LiB_3O_5 glass was prepared by fusing for 2 hours in a platinum (Pt) crucible in an air atmosphere at a temperature of 1200 K. After that, the melt was poured onto a metal substrate at room temperature and a glass block was obtained from which plates of 6×7×1.5 mm were cut. The surfaces of the samples were ground and polished.

Luminescence studies at T=8.6 K were carried out using synchrotron radiation at the Superlumi/P66 beamline of the PETRA III synchrotron facility at DESY in Hamburg [17]. A primary 2 m long monochromator with a spectral resolution of 4 Å was used to select the spectral range of synchrotron radiation for luminescence excitation. Luminescence spectra were recorded and analyzed using an ANDOR Kymera monochromator with a spectral resolution of 2 Å, a Newton 920 CCD camera, and a Hamamatsu R6358 photomultiplier tube. The Lorentzian spectral lines profile has been used for emission spectra decomposition.

3. Results and discussion

The luminescence spectra of undoped LiB_3O_5 glass were recorded under excitation by synchrotron radiation with an energy of 22.2 eV (56 nm) and 7.1 eV (175 nm). The first spectrum recorded at excitation E_{exc}= 22.2 eV, shown in Fig. 1, is an intense emission

spectrum with a maximum of 3.3 eV and covers a wide band ranging from 2.25 eV to 4.25 eV. As can be seen from Fig. 1, this spectrum is complex and decomposes into three elementary components with maxima at 2.6 eV, 3.1 eV, and 3.4 eV.

The second spectrum, with a maximum of 2.9 eV after excitation by photons with E_{exc}=7.1 eV, has a slightly different appearance (Fig. 2). It also covers a fairly wide range but has a much lower intensity. This spectrum is also complex but has only two elementary components with maxima at 2.9 eV and ~2.2 eV.

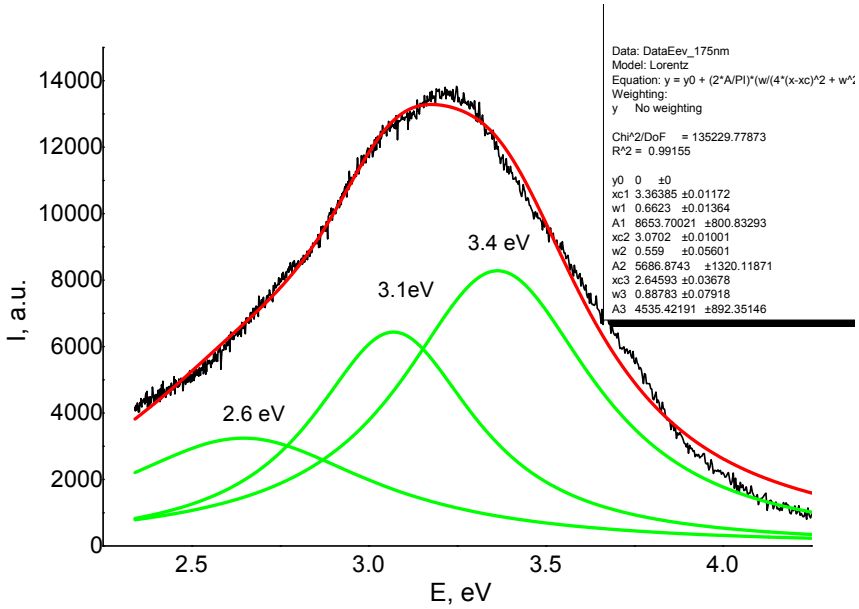

Fig. 1. Emission spectra of undoped LiB_3O_5 glass recorded at λ_{exc} = 56 nm (22.2 eV) and T=8.6 K. Black curve – experimental spectrum, green curves – Lorentzian elementary spectral lines, red curve – approximated spectrum.

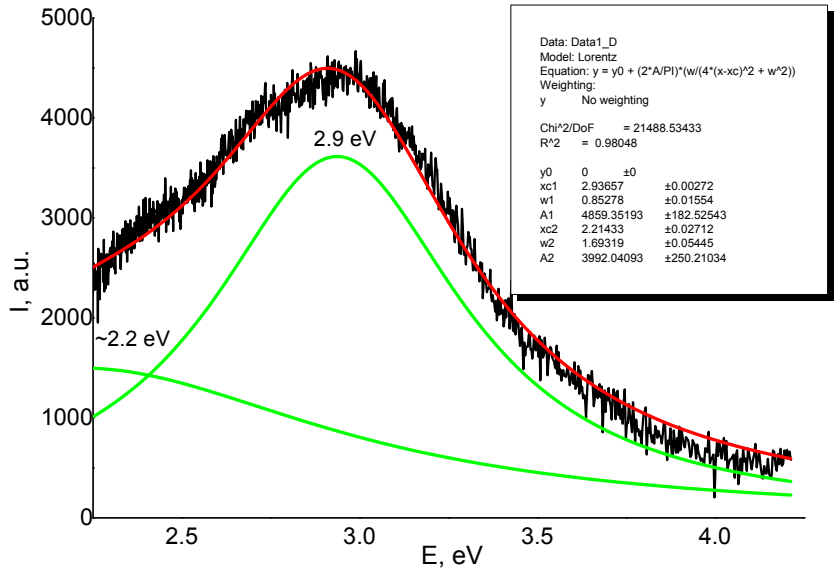

Fig. 2. Emission spectra of undoped LiB_3O_5 glass, recorded at λ_{exc}=175 nm (7.1 eV) and T=8.6 K. Black curve – experimental spectrum, green curves – Lorentzian elementary spectral lines, red curve – approximated spectrum.

Studies of excitation spectra showed that the 3.4 eV emission band is effectively excited by a broad band from 5.5 to 9.0 eV with a maximum in the range of 7.0 - 8.0 eV (Fig. 3). It is worth noting that the rapid increase in the excitation intensity (Fig. 3) coincides with the beginning of a rapid increase in the optical absorption in undoped LiB_3O_5 glass (Fig. 4).

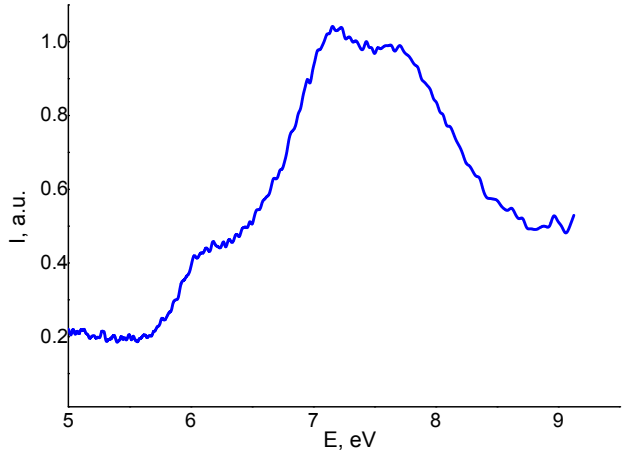

Fig. 3. The luminescence excitation spectrum of undoped LiB_3O_5 glass was recorded at λ_{mon} = 376 nm (3.3 eV) and T=8.6 K.

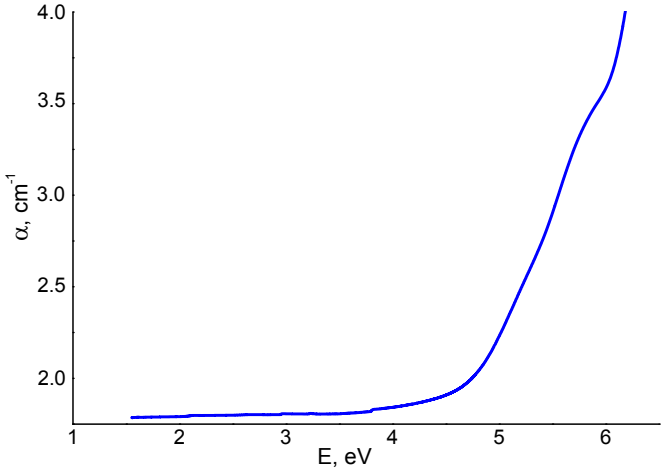

Fig. 4. Absorption spectra of undoped LiB_3O_5 glass at ambient temperature.

To interpret the results of our low-temperature luminescence studies of undoped LiB_3O_5 glass under the influence of synchrotron radiation, it is worth analyzing the published results of fundamental studies of undoped LiB_3O_5 single crystals [14-16]. To do this, it is first necessary to conduct a comparative analysis of the structural differences of the LiB_3O_5 compound in the ordered crystal state, where the long-range order exists, and in the amorphous state of glass, where the long-range order is absent.

Thus, the crystalline LiB_3O_5 has an orthorhombic crystal structure with the $Pna2_1$ space group and lattice parameters a=8.46 Å, b=5.13 Å, and c=7.38 Å [18]. In the structure of LiB_3O_5 crystal, two of the three boron atoms were threefold-coordinated by oxygen (BO_3), with B-O distances; 1) 0.13486, 0.1367, and 0.1396 nm (an average of 0.1370 nm) for one of

the B atoms; 2) 0.13564, 0.1369, and 0.1391 nm (an average of 0.1372 nm) for the other one B atoms. The remaining boron atoms were fourfold-coordinated by oxygen (BO_4) with a B-O distance of 0.1460, 0.1461, 0.1483, and 0.1489 nm (an average of 0.1473 nm). Thus, the generalized average B-O distance in the $(B_3O_7)^{5-}$ complex is 0.1405 nm. Lithium atoms were fourfold-coordinated by oxygen (LiO_4), with Li - O distances of 0.1979, 0.2005, 0.2013, and 0.2180 nm (an average of 0.2044 nm).

A completely different picture is observed when we obtain the LiB_3O_5 compound in the form of glass. It is known that glass has no long-range order, so its main constituent elements, boron-oxygen complexes $(B_3O_7)^{5-}$, are arranged rather chaotically but completely retain the close order between the constituent boron and oxygen atoms. However, the absence of long-range order in the glass still slightly affects the average distances between atoms in the $(B_3O_7)^{5-}$ complex. However, significant changes occur, especially with the average distances in the LiO_4 tetrahedron. This was demonstrated by the results of experimental studies of the structure of LiB_3O_5 glasses reported in [19]. It is shown that the structure of LiB_3O_5 glasses has an average B-O distance of 0.144 nm, which is quite slightly higher than the generalized average value of the B-O distance in a single crystal (0.1405 nm). This excess may be due to the peculiarities of the LiB_3O_5 glass manufacturing technology, which requires significant melt overheating before subsequent sharp cooling, during which the melt structure freezes. In [20], it was experimentally shown that overheating in borate melts slightly changes the ratio of the concentrations of BO_4/BO_3 complexes in favor of BO_4. Thus, it can be confidently stated that due to the covalent B-O bonds, the structure of $(B_3O_7)^{5-}$ complexes practically does not change. Significant changes in the LiO_4 complex provide the chaotic structure of the glass due to the much weaker Li-O ionic bond, which is reflected in a significant increase in the average Li-O distance from 0.204 nm for a single crystal to 0.250 nm for glass.

These structural differences between LiB_3O_5 crystal and glass form the differences between their electronic structures. In crystalline LiB_3O_5, the electronic structure is characterized by highly localized bands with a direct gap of 7.37 eV, and the conduction band and the valence band are formed by the electronic states B2s, B2p, O2s, and O2p of the elemental complexes BO_3 and BO_4, i.e., actually formed by $(B_3O_7)^{5-}$ complexes [21], and, as detailed low-temperature studies of absorption spectra in [14] have shown, the band structure of the LiB_3O_5 crystal can be divided into overlapping subbands. Of course, the electronic states of Li2s and Li2p also partially contribute to the conduction band of LiB_3O_5 crystal.

The electronic structure of LiB_3O_5 glasses differs significantly due to the lack of translational symmetry. Therefore, the universal characteristics of electronic states, namely the distribution of electron energy density, are used to describe the electronic structure of disordered media such as glass. In this case, the long-wavelength shift of the absorption edge of glass compared with single crystals can be explained by the blurring of the electronic density of states. Moreover, the energy band model can still be applied to glass, but considering that direct interband transitions are prohibited, only indirect transitions and excitons can occur [22]. Accordingly, the absorption spectrum of the LiB_3O_5 glass (Fig. 4) differs significantly from that of a single crystal because it does not have a clearly defined absorption edge. This is typical for glassy samples because the glass structure lacks translational symmetry. However, due to the stability of $(B_3O_7)^{5-}$ complexes, it can be

assumed that some physical properties of LiB_3O_5 single crystals, in particular, luminescent properties, can be preserved in LiB_3O_5 glass, in particular, the formation of excitons in the glass structure [22] and their participation in the photoluminescence (PL).

Indeed, based on the results of studies of PL and photoexcitation, and taking into account the peculiarities of the band structure of LiB_3O_5 crystals, authors [14-16] proposed the following mechanism of low-temperature luminescence for the LiB_3O_5 crystal: a broadband PL with a maximum at 3.75-3.8 eV is due to intrinsic luminescence and occurs as a result of annihilation with the emission of self-localized excitons (STE). This mechanism was first proposed by the authors of [23] in 1986 to explain low-temperature luminescence in single crystals of lithium borates.

Thus, it can be assumed with high probability that the proposed mechanism of low-temperature luminescence in undoped LiB_3O_5 single crystals is quite suitable for explaining luminescence in undoped LiB_3O_5 glasses. After all, the emission spectra (Fig. 1) of undoped LiB_3O_5 glass recorded at λ_{exc} = 56 nm (22.2 eV) and T = 8.6 K can be decomposed into three elementary components 2.6 eV, 3.1 eV, and 3.4 eV, similar to those obtained in [15,16] for a single crystal of LiB_3O_5 under X-ray excitation and a temperature of 80 K, although with slightly shifted maxima on the energy scale (3.0 eV, 3.6 eV and 4.2 eV). A similar analogy is also observed when comparing the PL spectra of undoped LiB_3O_5 single crystals at 9.6 K (E_{exc} = 6.3 eV) [16]. Undoped LiB_3O_5 glass under photon excitation at 7.1 eV and a temperature of 8.6 K (Fig. 2). The emission spectra are decomposed into two components in both cases. Still, if in crystals these two components, 3.3 eV and 2.7 eV, differ in different radiation lifetimes, then for glass, the 2.9 eV component and a very clear band with a probable maximum of ~2.2 eV are visible. The excitation spectrum of a single crystal of LiB_3O_5 is in the range of 7.5 - 9.0 eV at 9.6 K [16], and the excitation spectrum of LiB_3O_5 glass occupies a much larger range of 5.5 - 9.0 eV (Fig. 3), which is consistent with the absorption spectrum of glass (Fig. 4) and the differences in the structure of the electronic energy structures of the crystal and glass.

Thus, the above comparative analysis of the results of our studies with the results of studies of undoped LiB_3O_5 single crystals allows us to propose an emission mechanism of undoped LiB_3O_5 glass at low temperatures. When excited by photons with an energy of 22.2 eV, non-relaxed excitons of the molecular type are formed in the structure of undoped glass LiB_3O_5. Then, their migration occurs with subsequent autolocalization (STE formation) near various point defects in the glass structure. The emission bands of 2.6 eV, 3.1 eV, and 3.4 eV (Fig. 1) and the 2.9 eV component (Fig. 2) are most likely to arise as a result of annihilation with the emission of STE of different types, depending on the defect on which the exciton is localized. However, the 2.2 eV band (Fig. 2) may be responsible for oxygen or lithium vacancies in the LiO_4 complex.

4. Conclusion

Lithium triborate glass LiB_3O_5, due to its tissue-equivalent Z_{eff}, is maybe the most promising material for dosimetry in medical practice. This requires fundamental research of its physical properties, in particular, luminescence. The present work studied the low-temperature (8.6 K) luminescence of undoped LiB_3O_5 glass under excitation by synchrotron radiation (22.2 eV and 7.1 eV).

The emission spectrum recorded at 22.2 eV is decomposed into three elementary components: 2.6 eV, 3.1 eV, and 3.4 eV. In comparison, the one recorded at 7.1 eV is

decomposed into only two elementary components with maxima at 2.9 eV and in the 2.2 eV region. A comparative analysis of our results with the results of studies of the low-temperature luminescence of undoped LiB_3O_5 single crystals allowed us to propose a mechanism for the emission of undoped LiB_3O_5 glass at low temperatures, which is associated with the formation of unrelaxed molecular-type excitons, their migration, followed by the formation of STEs near various point defects in the glass structure. Accordingly, the emission bands of 2.6 eV, 3.1 eV, and 3.4 eV at 22.2 eV excitation are most likely to arise due to annihilation with the emission of different STEs, depending on the defect on which the exciton is localized. The STE formed at 7.1 eV excitation is localized on another defect, resulting in the appearance of an emission band with a maximum of 2.9 eV. The 2.2 eV band can be caused by oxygen or lithium vacancies in the LiO_4 complex.

Acknowledgments. This work was supported at the EURIZON project #ID70, funded by the European Union under grant agreement No.871072.

5. References

1. Adamiv, V. T., Burak, Y. V., Teslyuk, I. M., Antonyak, O. T., Moroz, I. E., & Malynych, S. Z. (2019). LiB_3O_5 pyroceramic for thermoluminescent dosimeters. *Ukrainian Journal of Physical Optics*, *20*(4), 151-167.
2. Saray, A. A., Kaviani, P., & Shahbazi-Gahrouei, D. (2021). Dosimetric characteristics of lithium triborate (LiB_3O_5) nanophosphor for medical applications. *Radiation Measurements*, *140*, 106502.
3. Wouter, C., Dirk, V., Paul, L., & Tom, D. (2017). A reusable OSL-film for 2D radiotherapy dosimetry. *Physics in Medicine & Biology*, *62*(21), 8441.
4. Ahmed, M. F., Eller, S. A., Schnell, E., Ahmad, S., Akselrod, M. S., Hanson, O. D., & Yukihara, E. G. (2014). Development of a 2D dosimetry system based on the optically stimulated luminescence of Al_2O_3. *Radiation Measurements*, *71*, 187-192.
5. Ahmed, M. F., Shrestha, N., Ahmad, S., Schnell, E., Akselrod, M. S., & Yukihara, E. G. (2017). Demonstration of 2D dosimetry using Al_2O_3 optically stimulated luminescence films for therapeutic megavoltage x-ray and ion beams. *Radiation Measurements*, *106*, 315-320.
6. Al-Senan, R. M., & Hatab, M. R. (2011). Characteristics of an OSLD in the diagnostic energy range. *Medical Physics*, *38*(7), 4396-4405.
7. Yukihara, E. G., & Kron, T. (2020). Applications of optically stimulated luminescence in medical dosimetry. *Radiation Protection Dosimetry*, *192*(2), 122-138.
8. Yukihara, E. G., McKeever, S. W., & Akselrod, M. S. (2014). State of art: Optically stimulated luminescence dosimetry–Frontiers of future research. *Radiation Measurements*, *71*, 15-24.
9. Sholom, S., & McKeever, S. W. S. (2023). Silver molecular clusters and the properties of radiophotoluminescence of alkali-phosphate glasses at high dose. *Radiation Measurements*, *163*, 106924.
10. Gustafson, T. D., Milliken, E. D., Jacobsohn, L. G., & Yukihara, E. G. (2019). Progress and challenges towards the development of a new optically stimulated luminescence (OSL) material based on MgB_4O_7: Ce, Li. *Journal of Luminescence*, *212*, 242-249.
11. Kananen, B. E., Maniego, E. S., Golden, E. M., Giles, N. C., McClory, J. W., Adamiv, V. T., Burak, Ya.V. & Halliburton, L. E. (2016). Optically stimulated luminescence (OSL) from Ag-doped $Li_2B_4O_7$ crystals. *Journal of Luminescence*, *177*, 190-196.
12. Adamiv, V., Burak, Y., Volodko, N., Dutchak, U., Izo, T., Teslyuk, I., & Luchechko, A. (2024). Effect of gamma-irradiation on the photoluminescence of silver-doped lithium triborate glass. *Applied Optics*, *63*(10), 2630-2635.
13. Kitagawa, Y., Yukihara, E. G., & Tanabe, S. (2021). Development of Ce^{3+} and Li^{+} co-doped magnesium borate glass ceramics for optically stimulated luminescence dosimetry. *Journal of Luminescence*, *232*, 117847.
14. Ivanov, V. Y., Kuznetsov, A. Y., Ogorodnikov, I. N., Pustovarov, V. A., & Kruzhalov, A. V. (1995). Luminescence of lithium triborate crystals under high intensity synchrotron radiation. *Nuclear Instruments and Methods in Physics Research Section A: Accelerators, Spectrometers, Detectors and Associated Equipment*, *359*(1-2), 339-341.
15. Ogorodnikov, I. N., Pustovarov, V. A., Porotnikov, A. V., & Kruzhalov, A. V. (1998). A polarized fast luminescence of LiB_3O_5 single crystals excited by synchrotron radiation. *Nuclear Instruments and Methods in Physics Research Section A: Accelerators, Spectrometers, Detectors and Associated Equipment*, *405*(2-3), 403-407.

16. Ogorodnikov, I. N., Isaenko, L. I., Kruzhalov, A. V., & Porotnikov, A. V. (2001). Thermally stimulated luminescence and lattice defects in crystals of alkali metal borate LiB_3O_5 (LBO). *Radiation Measurements*, *33*(5), 577-581.
17. https://photon-science.desy.de/facilities/petra_iii/beamlines/p66_superlumi/i ndex_eng.html.
18. Hoppe, R. (1978). ber Borati der Alkalimetalle. II. Zur Kenntnis von LiB_3O_5 [1]. *Zeitschrift für Anorganische und Allgemeine Chemie*, *439*(1), 71-79.
19. Padlyak, B. V., Mudry, S. I., Kulyk, Y. O., Drzewiecki, A., Adamiv, V. T., Burak, Y. V., & Teslyuk, I. M. (2012). Synthesis and X-ray structural investigation of undoped borate glasses. *Materials Science-Poland*, *30*, 264-273.
20. Osipov, A. A., & Osipova, L. M. (2010). Structural studies of $Na_2O–B_2O_3$ glasses and melts using high-temperature Raman spectroscopy. *Physica B: Condensed Matter*, *405*(23), 4718-4732.
21. Xu, Y. N., & Ching, W. Y. (1990). Electronic structure and optical properties of LiB3O5. *Physical Review B*, *41*(8), 5471.
22. Moustafa, Y. M., Hassan, A. K., El-Damrawi, G., & Yevtushenko, N. G. (1996). Structural properties of V_2O_5-Li_2O-B_2O_3 glasses doped with copper oxide. *Journal of Non-Crystalline Solids*, *194*(1-2), 34-40.
23. Antonyak, O. T., Burak, Y. V., Lyseiko, I. T., Pidzyrailo, N. S., & Khapko, Z. A. (1986). Luminescence of $Li_2B_4O_7$ crystals. *Optics and Spectroscopy*, *61*(3), 345-347.

V. Adamiv, Ya. Burak, I. Medvid, I. Koflyuk, U. Dutchak, I. Teslyuk, T. Izo, R. Gamernyk. (2025). Low-Temperature Luminescence of LiB_3O_5 Glass with a Human Body Tissue-Equivalent Effective Atomic Number**.** *Ukrainian Journal of Physical Optics*, *26*(1), 01001 – 01008.
doi: 10.3116/16091833/Ukr.J.Phys.Opt.2025.01001

Анотація*. Проведено дослідження низькотемпературної (8,6 К) люмінесценції нелегованого скла LiB_3O_5 при збудженні синхротронним випромінюванням (22,2 еВ і 7,1 еВ). Проведено порівняльний аналіз отриманих результатів з опублікованими іншими авторами результатами досліджень низькотемпературної люмінесценції нелегованих монокристалів LiB_3O_5. У результаті запропоновано механізм випромінювання нелегованого скла LiB_3O_5 при низьких температурах, який пов'язаний з утворенням нерелаксованих екситонів молекулярного типу, їх міграцією з подальшим утворенням автолокалізованих екситонів поблизу точкових дефектів і їх анігіляцією.*

Ключові слова*: триборатне скло літію, фотолюмінесценція, синхротронне випромінювання, дозиметрія*